Supporting Information

Amorphous versus nanocrystalline RuO_2 electrocatalysts: Activity and stability for oxygen evolution reaction in sulfuric acid

Kosuke Beppu, [a] Kazuki Obigane, [a] and Fumiaki Amano *[a]

[a]*Department of Applied Chemistry for Environment, Graduate School of Urban Environmental Sciences, Tokyo Metropolitan University, 1-1 Minami-Osawa, Hachioji, Tokyo 192-0397, Japan.*

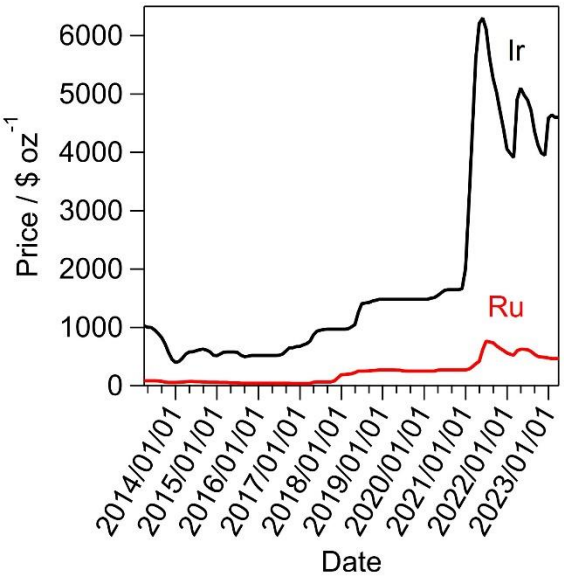

Figure S1 Ir and Ru price changes over the past 10 years. The data were obtained from http://www.platinum.matthey.com/prices/price-charts.

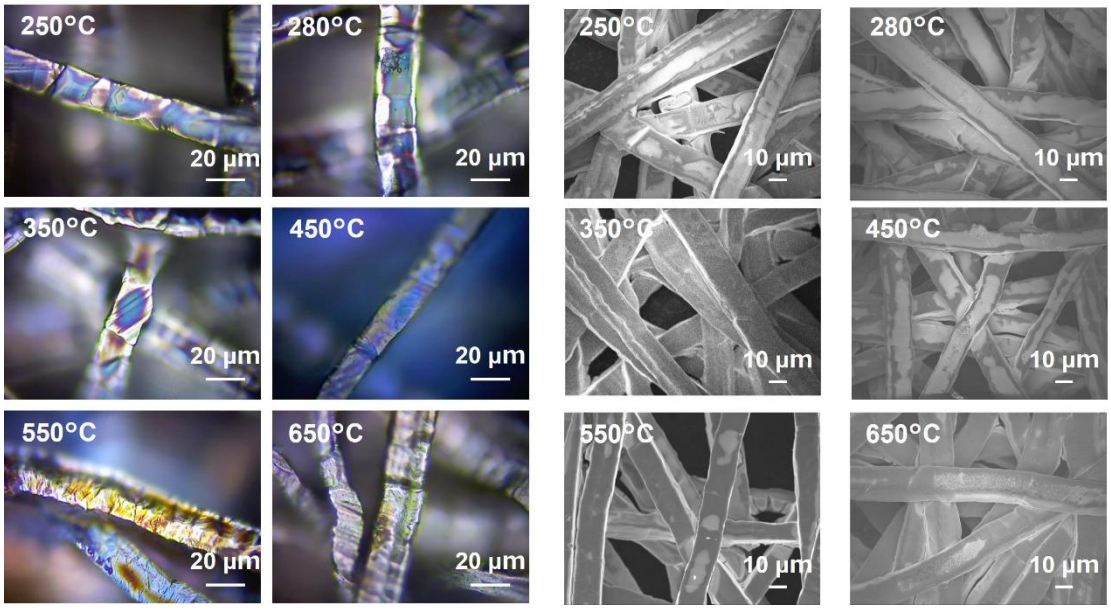

Figure S2 Optical micrographs (left) and low magnification SEM images (right) of RuO_2/Ti-felt(x) samples.

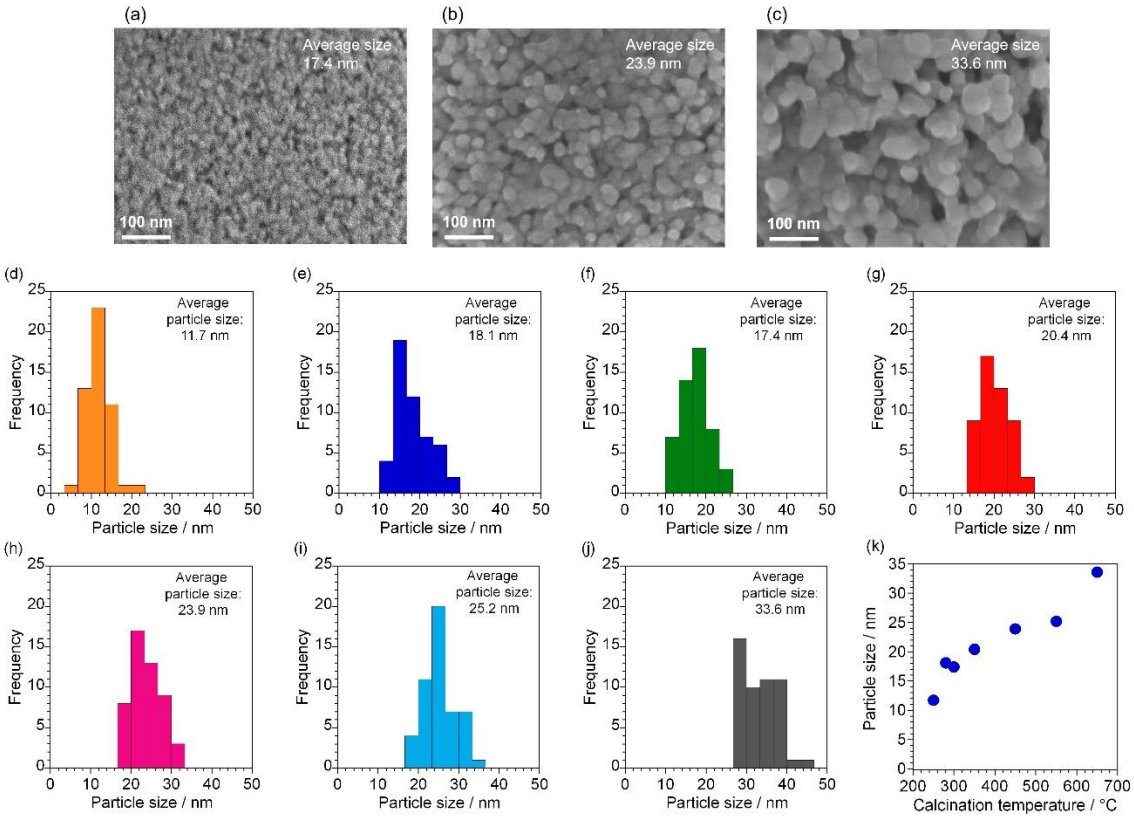

Figure S3 Surface SEM images of (a) RuO_2/Ti-felt(300), (b) RuO_2/Ti-felt(450) and (c) RuO_2/Ti-felt(650) electrocatalysts. (d–j) Particle size distributions of RuO_2 in RuO_2/Ti-felt(x) samples estimated from SEM images; (d) RuO_2/Ti-felt(250), (e) RuO_2/Ti-felt(280), (f) RuO_2/Ti-felt(300), (g) RuO_2/Ti-felt(350), (h) RuO_2/Ti-felt(450), (i) RuO_2/Ti-felt(550) and (j) RuO_2/Ti-felt(650). (k) Average particle size in RuO_2/Ti-felt(x) samples as a function of calcination temperature.

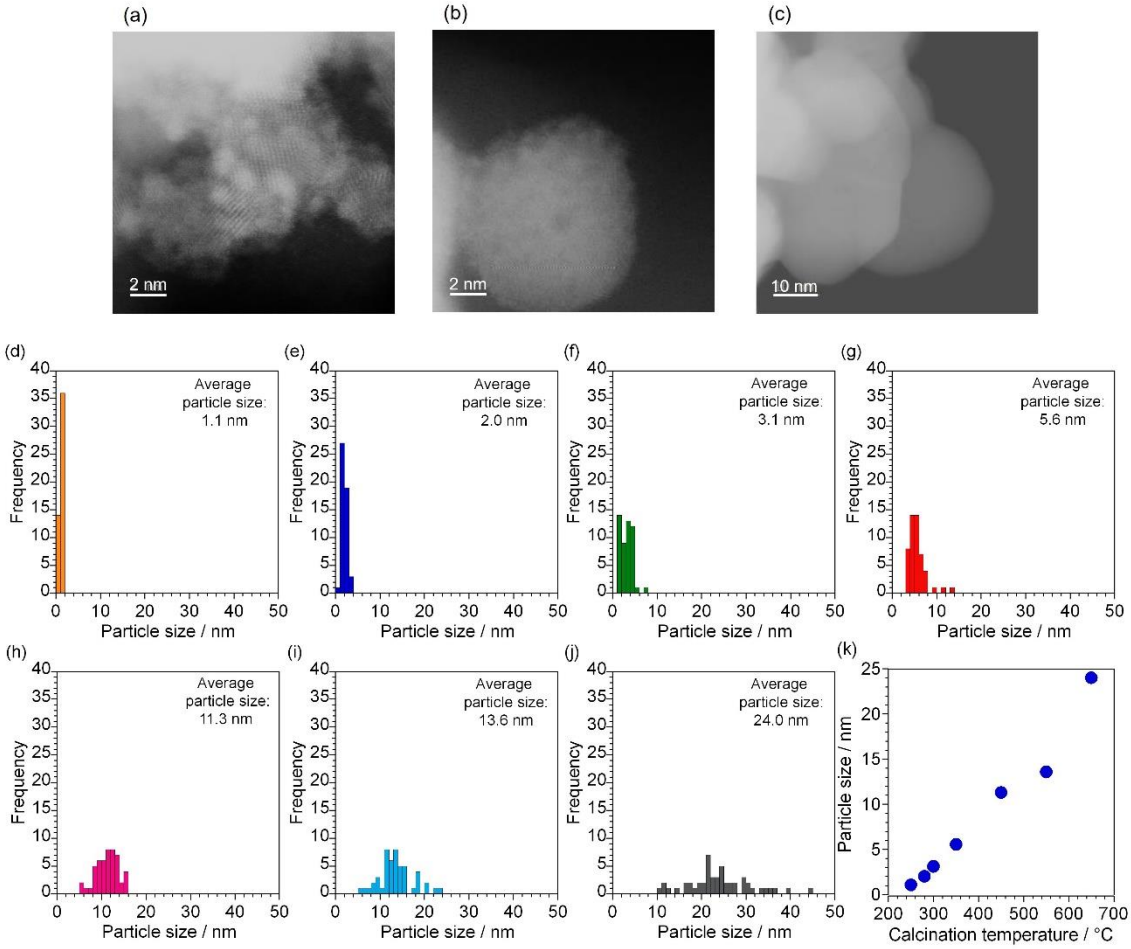

Figure S4 STEM images of (a) RuO_2/Ti-felt(300), (b) RuO_2/Ti-felt(450) and (c) RuO_2/Ti-felt(650) electrocatalysts. (d–j) Particle size distributions of RuO_2 in RuO_2/Ti-felt(x) estimated from STEM images; (d) RuO_2/Ti-felt(250), (e) RuO_2/Ti-felt(280), (f) RuO_2/Ti-felt(300), (g) RuO_2/Ti-felt(350), (h) RuO_2/Ti-felt(450), (i) RuO_2/Ti-felt(550) and (j) RuO_2/Ti-felt(650). (k) Average particle size in RuO_2/Ti-felt(x) samples as a function of calcination temperature.

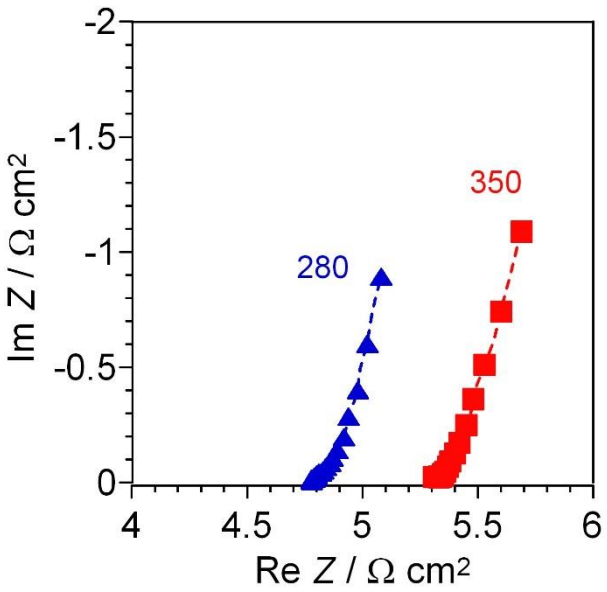

Figure S5 EIS spectra of RuO_2/Ti-felt(280) and RuO_2/Ti-felt(350) electrocatalysts. Data were obtained at 0.26 V vs. RHE from 10 to 10000 Hz.

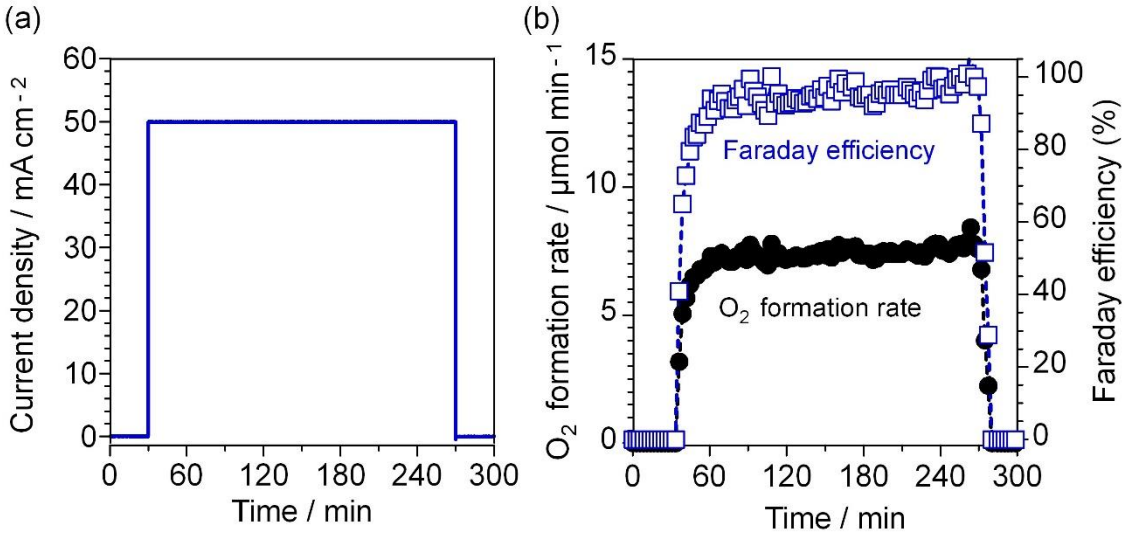

Figure S6 (a) Time course of current density for O_2 gas detection for 4 h. (b) The rate of O_2 gas evolution and Faraday efficiency of O_2 production. The current density was set at zero for 30 min before and 30 min after a 4 h CP experiment at 50 mA cm^{-2}.

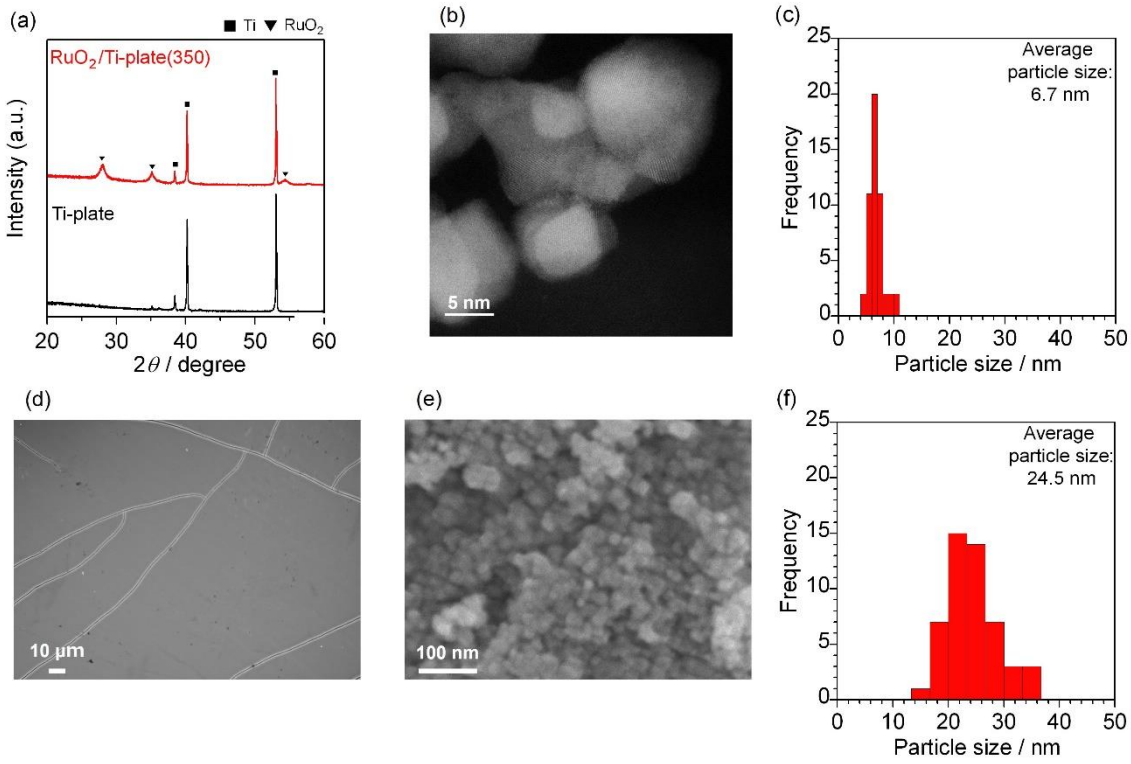

Figure S7 Characterisation of the RuO_2/Ti-plate(350) electrocatalyst. (a) XRD patterns. (b) STEM image. (c) Particle size distribution of RuO_2/Ti-plate(350) estimated by STEM. (d) Low and (e) high magnification SEM images. (f) Particle size distribution of RuO_2/Ti-plate(350) estimated by SEM.

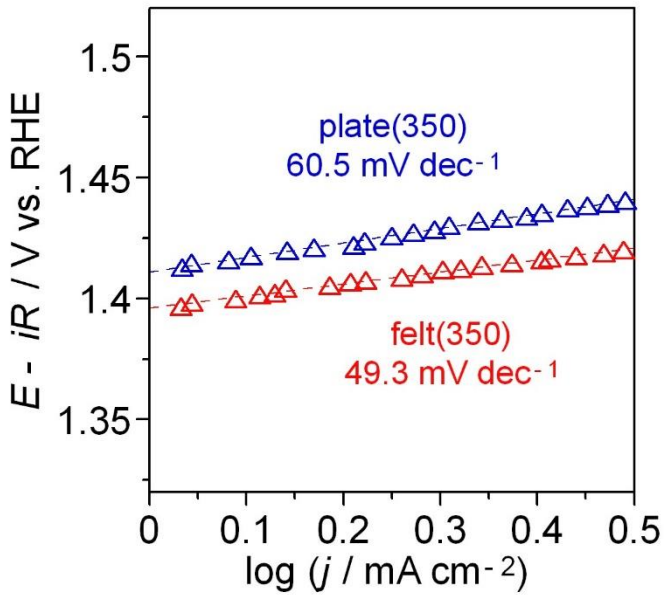

Figure S8 Tafel plots and slopes of *iR*-corrected OER activities of RuO_2/Ti-felt(350) and RuO_2/Ti-plate(350) electrocatalysts. Dashed lines are the fitting results.

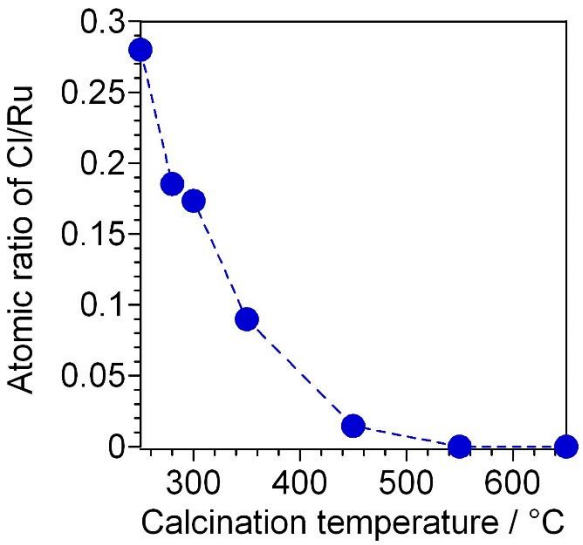

Figure S9 Effect of calcination temperature on the surface Cl/Ru ratio obtained from XPS spectra.

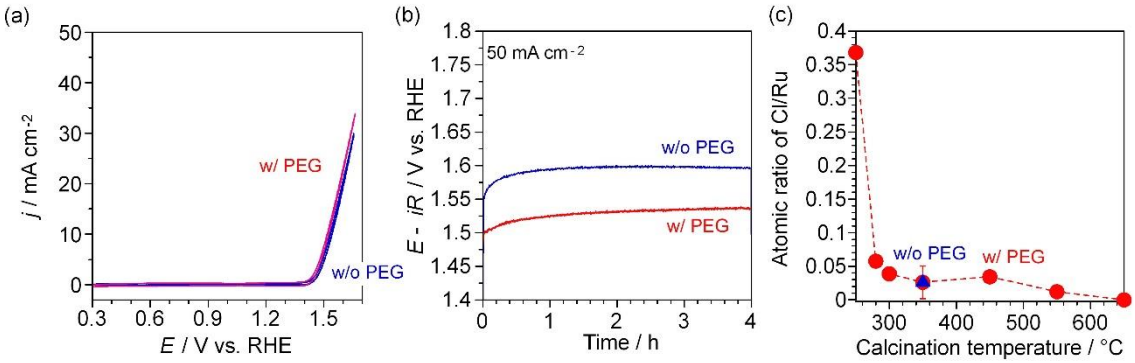

Figure S10 Comparative OER performance of RuO_2/Ti-felt(350) electrocatalyst using the precursor with (red) and without (blue) PEG. (a) CV at 10 mV s^{-1}. (b) Chronopotentiometry at 50 mA cm^{-2}. (c) Atomic ratio of Cl/Ru obtained from XRF spectra.

Table S1 Comparison of OER activity with that of previously reported electrocatalysts.

Samples	η at 10 mA cm^{-2} [mV]	Tafel slope [mV dec^{-1}]	O_2 Faraday efficiency	Electrolyte	Reference
RuO_2/ Ti felt(350)	215	49.3	96 ± 3% (50 mA cm^{-2})	0.1 M H_2SO_4	This work
FeCoNiIrRu	241	153	–	0.5 M H_2SO_4	38
Ni-RuO_2	214	42.6	–	0.1 M $HClO_4$	40
SrRuIrO	190	39	–	0.5 M H_2SO_4	18
$Y_2Ru_2O_7$	337	40	95−100%(1.56 V vs. RHE)	0.1 M $HClO_4$	26
$SnRuO_x$	194	38.2	–	0.1 M H_2SO_4	39
IrO_x	340	–	93% (10 mA cm^{-2})	1 M H_2SO_4	34
commercial-RuO_2	370	–	–	0.5 M H_2SO_4	39
amorphous-RuO_2	280	–	92% (10 mA cm^{-2})	1 M H_2SO_4	34